Mon. Not. R. astr. Soc. (1989) **238,** 407–416

Simulations of satellite orbital decay

Lars Hernquist and Martin D. Weinberg *Institute for Advanced Study, Princeton, NJ 08540, USA*

Accepted 1988 November 29. Received 1988 November 8; in original form 1988 June 27

Summary. The orbital decay of satellites around spherical galaxies is studied numerically using both self-consistent and semi-restricted N-body methods. The inferred sinking rates are in good agreement with analytic predictions from a linear perturbation analysis.

In particular, we verify that the orbital decay is strongly suppressed if the self-gravity of the response is included, in disagreement with other recent discussions of this problem. We suggest that the discrepancy can be traced to misuse of the term 'non-self-gravitating'.

Finally, we demonstrate that the loss of orbital angular momentum by the satellite is *not* a local process.

1 Introduction

The interaction of a large galaxy with its system of satellites can have a number of observable consequences. This is especially true for discs, which can undergo large-scale morphological changes in response to the accretion of even low-mass companions. Such events may be responsible for the growth of normal and/or boxy bulges, the triggering of nuclear activity and periods of enhanced star formation, grand design spiral structure, and vertical thickening of discs. The outcomes of encounters between ellipticals and smaller galaxies, though less spectacular, are almost as diverse. Cannibalism may account for ellipticals containing anomalous amounts of gas or dust, shells, multiple nuclei, X-structures, and counter-rotating cores.

In order to study such scenarios, it is necessary to understand the satellite's orbital evolution. In general, the accretion of satellites by a large galaxy is a direct consequence of dynamical friction. Depending on the orbital radii of the satellites and the structure of galaxian haloes, satellite orbits may not be stable over a Hubble time. Using an order-of-magnitude estimate appropriate for an isothermal halo, Tremaine (1981) computed that a galaxy such as the Milky Way could have accreted up to 10 per cent of its mass in the form of small companions since being formed. Given the potential importance of cannibalism, it is natural to investigate the decay of satellite orbits around various mass distributions in some detail.

Most previous studies have relied on the use of particle simulations. Lin & Tremaine (1983) used a semi-restricted N-body technique to examine the dependence of decay rates on the

orbital geometry and parameters associated with the satellite and primary galaxy. White (1983) subsequently noted that the sinking times inferred by Lin & Tremaine could be subject to errors of factors of ~2–3, because of the approximate nature of their method. However, self-consistent studies by Bontekoe & van Albada (1987; hereafter BvA) failed to substantiate White's claim, and suggested, rather, that the self-gravity of the response of the primary is not an important factor in determining the decay rates. Prompted by BvA's simulations, Zaritsky & White (1988, hereafter ZW) recently re-examined the sinking-satellite problem using a variety of self-consistent algorithms. They concluded that the self-gravity of the response is unimportant.

A different approach has been taken by Weinberg (1986, 1989) who calculates the response and sinking times analytically, using linear perturbation theory. For present purposes, his most relevant findings are:

(i) the response is always global, although a simple expression such as that derived by Chandrasekhar (1943) may, in some situations, provide the correct scalings,

(ii) the self-gravity of the response will increase the sinking time by factors of ~2–3.

In an attempt to clarify the present situation, we examine the decay of satellite orbits around a spherical galaxy using the model considered by BvA and ZW, with fully self-consistent and semi-restricted methods. Our results indicate that the self-gravity of the response is an important ingredient in the dynamical friction process, contrary to the conclusions expressed by BvA and ZW. We emphasize, however, that this disagreement is mainly over the interpretation of the term 'non-self-gravitating' and *not* the reliability of the simulations.

In the following section we describe our method in some detail. Numerical results are presented in Section 3. Finally, conclusions and a discussion follow in Section 4.

2 Method

2.1 PARAMETERS AND UNITS

In order to facilitate comparisons with other numerical studies, we use the primary model chosen by BvA and ZW. The galaxy is an $n=3$ polytrope, with mass $M=2$ and radius $R=1$, and the unit of time is fixed by setting $G=1$. The satellite is modelled as a rigid Plummer sphere with density profile

$$\rho(r)=\frac{3m_s}{4\pi}\frac{1}{r_c^3}\frac{1}{[1+(r/r_c)^2]^{5/2}}\,. \tag{1}$$

Following BvA and ZW and unless otherwise stated, we take the satellite mass, m_s, to be $m_s=0.2$, and the satellite scale-length, r_c, to be $r_c=0.1$. Thus, the mass ratio is usually $M:m_s=10:1$ and the ratio of the total size of the primary to the satellite scale-length is always $R:r_c=10:1$.

In all cases, the orbit of the satellite is initially circular. We vary the initial radius of the satellite orbit, $r_s(0)$, in order to examine the sensitivity of the decay rate to transient responses in the primary. Typically, $r_s(0)=1$, 1.2, or 1.5. For the runs with $r_s(0)>1$, we measure the decay time from the instant at which the satellite reaches the edges of the galaxy, $r_s=1$.

2.2 SELF-CONSISTENT METHOD

The self-consistent simulations performed by BvA and ZW were obtained using expansion techniques. In order to test the dependence of the results on the method itself, our self-gravitat-

ing runs were performed using a hierarchical tree algorithm (Barnes 1986; Barnes & Hut 1986).

In the hierarchical tree method, the particles are first organized into a nested hierarchy of cells and then multiple moments of each cell, up to a fixed order, are computed. The gravitational acceleration is obtained by allowing each particle to interact with various elements of the hierarchy, subject to a prescribed accuracy criterion. As a rule, the force from nearby particles is computed by directly summing the relevant two-body interactions. The influence of remote particles is included by evaluating the multipole expansions of the cells satisfying the accuracy requirements at the location of the particle on which to compute the acceleration.

Specifically, if

$$\frac{s}{d} \leq \theta, \tag{2}$$

where s is the size of a cell, d is the distance from the centre of mass of the cell to the particle in question, and θ is an input parameter which is typically of order unity, then the internal structure of the cell is ignored and the multipole approximation is used. The number of terms in the expansions is usually small compared with the number of particles in the corresponding cell and a significant improvement in efficiency is realized. The use of a tree data structure to manipulate the hierarchy reduces the operations count per step from $\sim O(N^2)$, which would result from a direct sum over *all* particles, to $\sim O(N \log N)$. In principle, then, the hierarchical tree method allows for the use of a large N, which is desirable in the case of satellite orbital decay to minimize relaxation effects and any associated numerical 'viscosity' (e.g. Lin & Tremaine 1983).

The free parameters in the self-consistent simulations are the two-body softening length, ε, the particle number, N, the time step, Δt, and the accuracy of the force computation, which is determined by θ and the number of terms in the multipole expansions. The sensitivity of the evolution of the satellite orbits to each of these quantities was studied in order to establish that a converged solution had been obtained.

The satellite and particles comprising the galaxy always interact directly with a softening length equal to the scale-length of the satellite, r_c. Since, typically, $r_c \gg \varepsilon$, the individual particles effectively interact with the satellite as if they were point-like. For definiteness, the equations of motion are

$$\ddot{\mathbf{r}}_i = -\sum_{j=1}^{\mathcal{N}_i} \phi_{ij} - \frac{m_s(\mathbf{r}_i - \mathbf{r}_s)}{[(\mathbf{r}_i - \mathbf{r}_s)^2 + r_c^2]^{3/2}} \quad i = 1, \ldots, N \tag{3}$$

$$\ddot{\mathbf{r}}_s = -\sum_{j=1}^{N} \frac{m_j(\mathbf{r}_s - \mathbf{r}_j)}{[(\mathbf{r}_j - \mathbf{r}_s)^2 + r_c^2]^{3/2}}, \tag{4}$$

where m_j is the mass of each particle, $\mathcal{N}_i$ is the number of cells and particles that interact with particle i, and the ϕ_{ij} are the particle–cell and particle–particle interaction potentials.

2.3 SEMI-RESTRICTED METHOD

The non-self-gravitating simulations were performed using a variation of the semi-restricted N-body technique introduced by Lin & Tremaine (1983). The potential for each particle is determined from the Lane–Emden equation, with polytropic index $n = 3$. The potential field is

fixed in time and is not allowed to move spatially, which is the appropriate numerical analogue of the non-self-gravitating analysis performed by Weinberg (1986, 1989).

The only numerical parameters in this case are N and Δt. Again, the satellite and galaxy particles interact directly and the equations of motion are

$$\ddot{\mathbf{r}}_i = -\nabla\Phi(\mathbf{r}_i, t) - \frac{m_s(\mathbf{r}_i - \mathbf{r}_s)}{[(\mathbf{r}_i - \mathbf{r}_s)^2 + r_c^2]^{3/2}} \quad i = 1, \ldots, N \tag{5}$$

$$\ddot{\mathbf{r}}_s = -\sum_{j=1}^{N} \frac{m_j(\mathbf{r}_s - \mathbf{r}_j)}{[(\mathbf{r}_j - \mathbf{r}_s)^2 + r_c^2]^{3/2}}, \tag{6}$$

where Φ is the exact expression for the potential of an $n = 3$ polytrope. Values of $\nabla\Phi$ are obtained from a look-up table.

2.4 DETAILS

All simulations discussed in this paper were performed on the CRAY XMP-48 at the Pittsburgh Supercomputing Center. The majority of the self-consistent models were evolved using the tree code described by Hernquist (1987, 1988), which is not completely vectorized. A *fully* vectorized version, identical in all other respects to the original code, was used for some of the simulations. The procedure used to vectorize the tree traversals, which is described by Hernquist (1989), leads to an improvement in the overall efficiency of the method by a factor of ~ 2–3, implying a total speed-up of a factor of ~ 400–500 on an XMP compared to a VAX 11/780 or SUN 3/50. The semi-restricted code is also fully vectorized and proved to be highly efficient, allowing us to routinely use $N \sim 10^5$.

3 Results

3.1 SINKING RATES

An example of the sinking curves found by the methods outlined in Section 2 is shown in Fig. 1 (solid curves), where they are compared with the corresponding results from Weinberg (1989) (dashed curves). For the self-gravitating model, we plot the distance from the satellite to the centre of mass of the particle distribution as a function of time. In the non-self-consistent case, we plot the distance of the satellite from the origin of the coordinate system which coincides with the centre of the fixed potential for all time.

The parameters for the self-consistent model in Fig. 1 were $N = 20\,000$; $\theta = 0.95$; $\Delta = 0.01$, and $\varepsilon = 0.01$. Terms up to, and including, quadrupole order were included in the multipole expansions, implying typical errors in the acceleration on each particle, relative to a full direct sum, of order a few tenths of 1 per cent. Over the course of the simulation, the change in total energy was approximately 0.55 per cent, while the change in angular momentum was approximately 0.47 per cent. For the semi-restricted simulation shown in Fig. 1, the total number of particles was $N = 80\,000$ and the time step was again $\Delta t = 0.01$. Since the particles do not interact with one another on an individual basis, the time step in this case is not limited by the particle density.

The sinking rate inferred from our simulation is in excellent agreement with that obtained by both BvA and ZW; for the same value of N, decay times agree to ≈ 2 per cent. However, the sinking time implied by the analytic calculation is somewhat larger than that obtained numerically. The times for the satellite to reach $r_s = 0.2$ differ by nearly 50 per cent. Speculat-

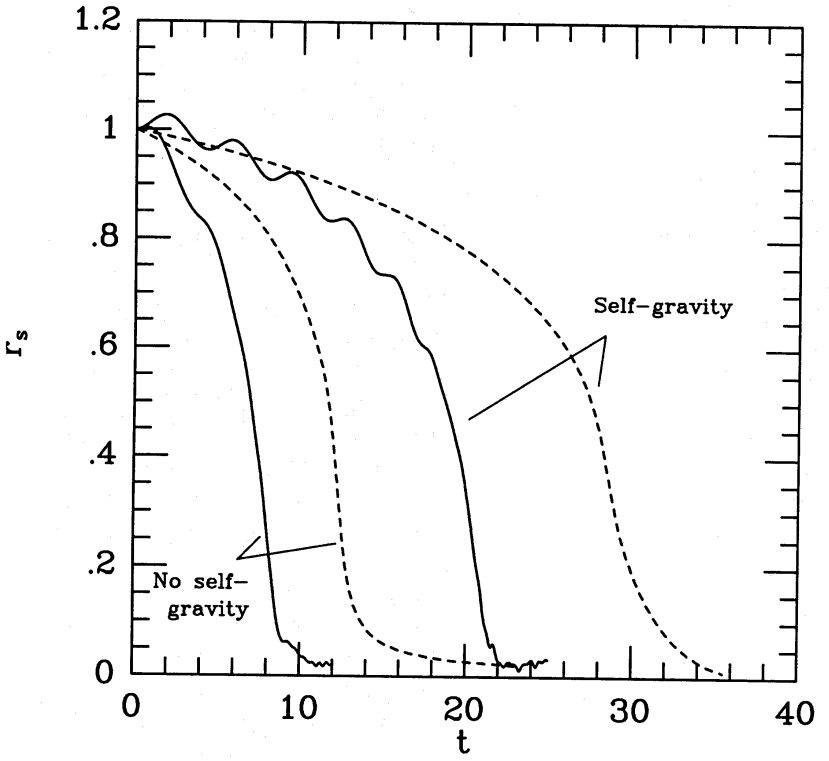

Figure 1. Sinking curves for fully self-gravitating and non-self-gravitating simulations (solid). Also shown are the corresponding curves from the analytic calculations of Weinberg (1988) (dashed).

ing that this might be attributable to non-linear and/or time-dependent effects which are not included in the analytic calculations, we performed a number of non-self-gravitating simulations with satellites of increasingly smaller masses. In the linear regime the decay time scales exactly as $\tau_{\rm decay} \propto 1/m_{\rm s}$. The product $\tau_{\rm decay} m_{\rm s}/0.2$ is shown in Fig. 2 for satellites of varying mass, where we choose to define $\tau_{\rm decay}$ as the time for the satellite orbit to decay from $r_{\rm s}=1.0$ to $r_{\rm s}=0.2$. As is clear from this figure, non-linear effects are significant for $m_{\rm s} \gtrsim 0.05$. For smaller masses the inferred decay times appear to be converging to a scaled value within the error of the analytic prediction of ≈ 12.7.

Ideally, we would like to repeat the self-gravitating simulations with small $m_{\rm s}$ to verify that the discrepancy in this case is also due to non-linear and/or time-dependent effects. Unfortunately, the computational expense is prohibitive for the particle number required to minimize discreteness effects for the time-scales of interest. These issues might be more efficiently studied using a technique optimized for spherical distributions such as an expansion method. Nonetheless, we emphasize that the ratios of self-gravitating to non-self-gravitating decay times are nearly identical for both the linearized calculation and the simulation.

The robustness of the sinking curves in Fig. 1 to numerical effects was examined by varying other simulation parameters. For smaller N the decay times are slightly smaller than the models shown in Fig. 1, for both simulations with and without self-gravity. For example, the sinking time in a self-consistent model with $N=5000$, as typically adopted by BvA and ZW, is approximately 5 per cent shorter than that of the model in Fig. 1. Reducing the number of particles from 80 000 to 20 000 in the semi-restricted code also reduces the sinking time by about 5 per cent, compared with the corresponding curve in Fig. 1. Improving the accuracy of the force computation in the hierarchical tree calculation by reducing θ does not result in a noticeable change in the sinking curve.

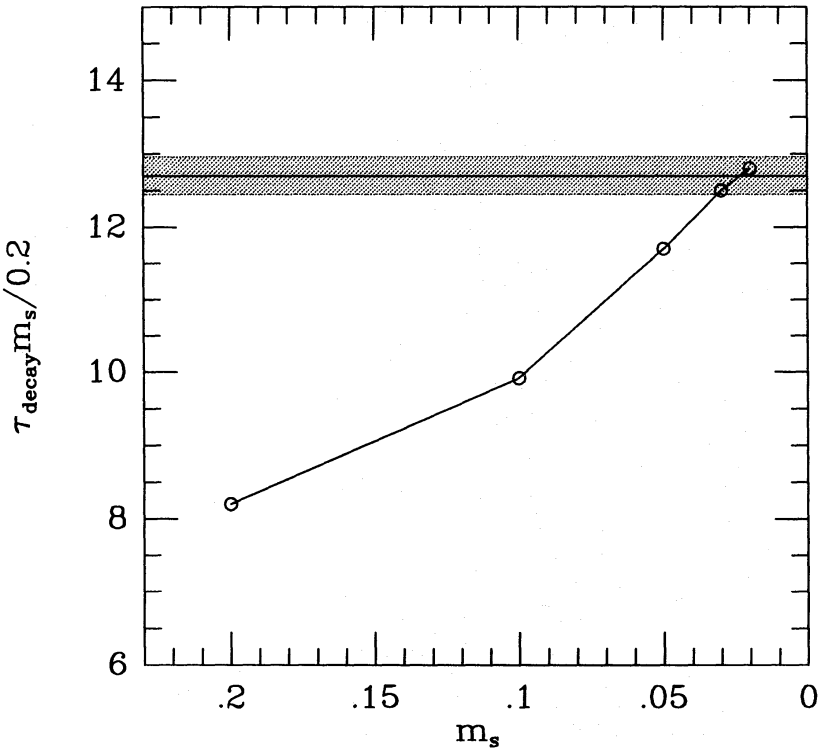

Figure 2. Scaled decay time as function of satellite mass for non-self-gravitating simulations (open circles). The analytic prediction (solid horizontal line) and its estimated error (shaded) are shown for comparison.

Finally, we considered the possible effects of transients by varying the initial radius of the satellite orbit. The differences in the inferred sinking times between the various runs are negligible. For example, in non-self-gravitating runs with $N=80\,000$, the times for the orbit to decay from $r_s=1.0$ to $r_s=0.2$ are $\tau_{decay}=8.1$, 8.0 and 8.0 for $r_s(0)=1$, 1.2, and 1.5, respectively. In the latter two cases, transients presumably have less effect on the orbital decay, since the satellite completes ~ 4 revolutions and ~ 20 revolutions, respectively, before reaching the galaxy.

3.2 GLOBAL RESPONSE

Linear perturbation theory demonstrates that the wake in the primary galaxy due to the satellite has global extent (Weinberg 1989). For example, the wake produced by a satellite orbiting at $r_s=1/3$ in a self-gravitating $n=3$ polytrope is shown in Fig. 3. The dipole ($l=1$) component is reduced by the barycentric motion and is roughly comparable to the sum of the higher-order ($l=2,3,4,\ldots$) terms in amplitude. The dipole term is responsible for the maximum density peak, located near $x=-0.1$, $y=-0.1$, while the secondary maximum, immediately behind the satellite, results from the higher-order components.

Given the agreement between the perturbation theory and the N-body experiments discussed above, we expect to see such wakes in the particle distributions. For the purpose of comparison with analytic results, we define the wake as the difference between the density observed in the simulation, $\rho_{\text{N-body}}$, and the density in absence of the satellite, ρ_0. Locating wakes is complicated by both discreteness effects and ambiguity in determining the proper origin for ρ_0, owing to barycentric motion. The latter difficulty is especially irksome.

To circumvent the difficulties arising from the barycentric motion, we opt to orbit two diametrically opposed satellites of equal mass, $m_s=0.03$. Their orbits are forced to remain

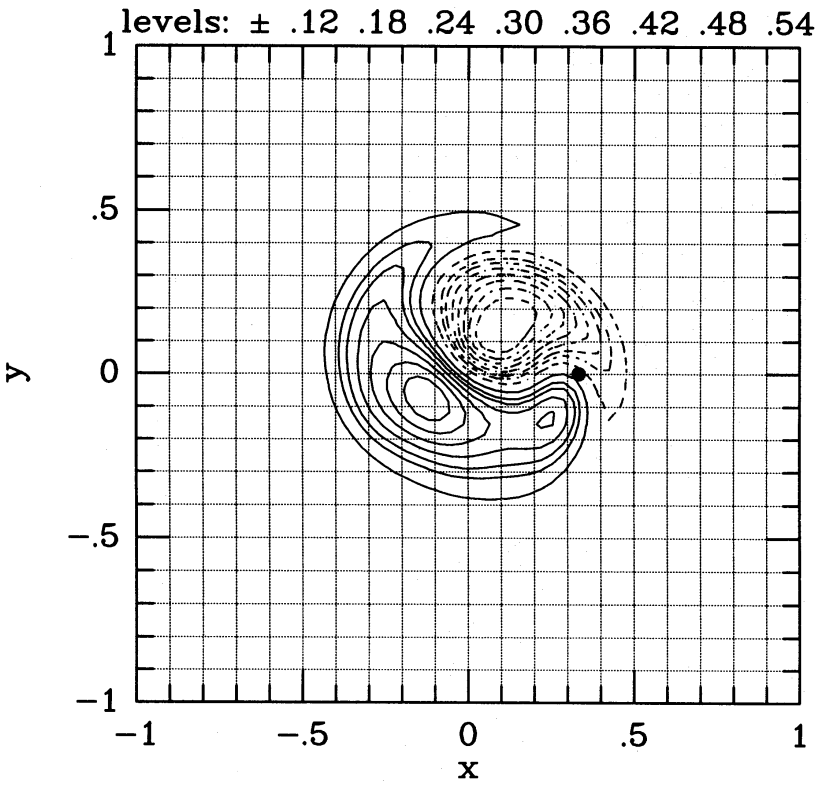

Figure 3. Wake derived from analytic calculation involving a single satellite of mass $m_s = 0.03$ and a self-gravitating primary. The position of the satellite is indicated by the solid circle. Solid (dashed) curves refer to overdensity (underdensity). The contour levels indicate the physical density at that location.

180° out of phase by averaging their accelerations at each time step. The centre of mass of the system then remains at the centre of the primary. Furthermore, this experiment is an excellent diagnostic of the nature of the response. If the response is local, the decay curves should be identical to the one-satellite case, assuming $m_s \ll M$. However, if the response is global, the wake must be even in azimuth, and all harmonic contributions with odd order ($l = 1, 3, 5, \ldots$) will vanish. According to analytic theory, the decay time should then increase by a factor of ~ 4.1 in the non-self-gravitating case. We do, in fact, find very good agreement with this prediction using the semi-restricted method. The decay curve is similar in shape to Fig. 1, but $\tau_{\rm decay}$ increases by a factor of 3.6, demonstrating the global nature of the response.

The predicted wake in the orbital plane is shown in Fig. 4(a) for a non-self-gravitating primary. We compute the wake from the particle distribution by performing a harmonic decomposition in spherical harmonics $Y_{\rm lm}$ and spherical Bessel functions j_n up to orders $l = 4$, $n = 4$; the result is shown in Fig. 4(b). The morphology and amplitudes of the two wakes agree reasonably well. The differences are consistent with fluctuation noise, the level of which was established by applying the harmonic decomposition routine to N-particle realizations of pure multipoles.

4 Discussion and conclusions

The agreement between the numerical simulations and the analytic decay curves provides a welcome check on both techniques. In addition, the agreement between the self-gravitating decay curve shown in Fig. 1 and those computed earlier by BvA and ZW using other N-body techniques demonstrates that the hierarchical tree method is a viable tool for evolving

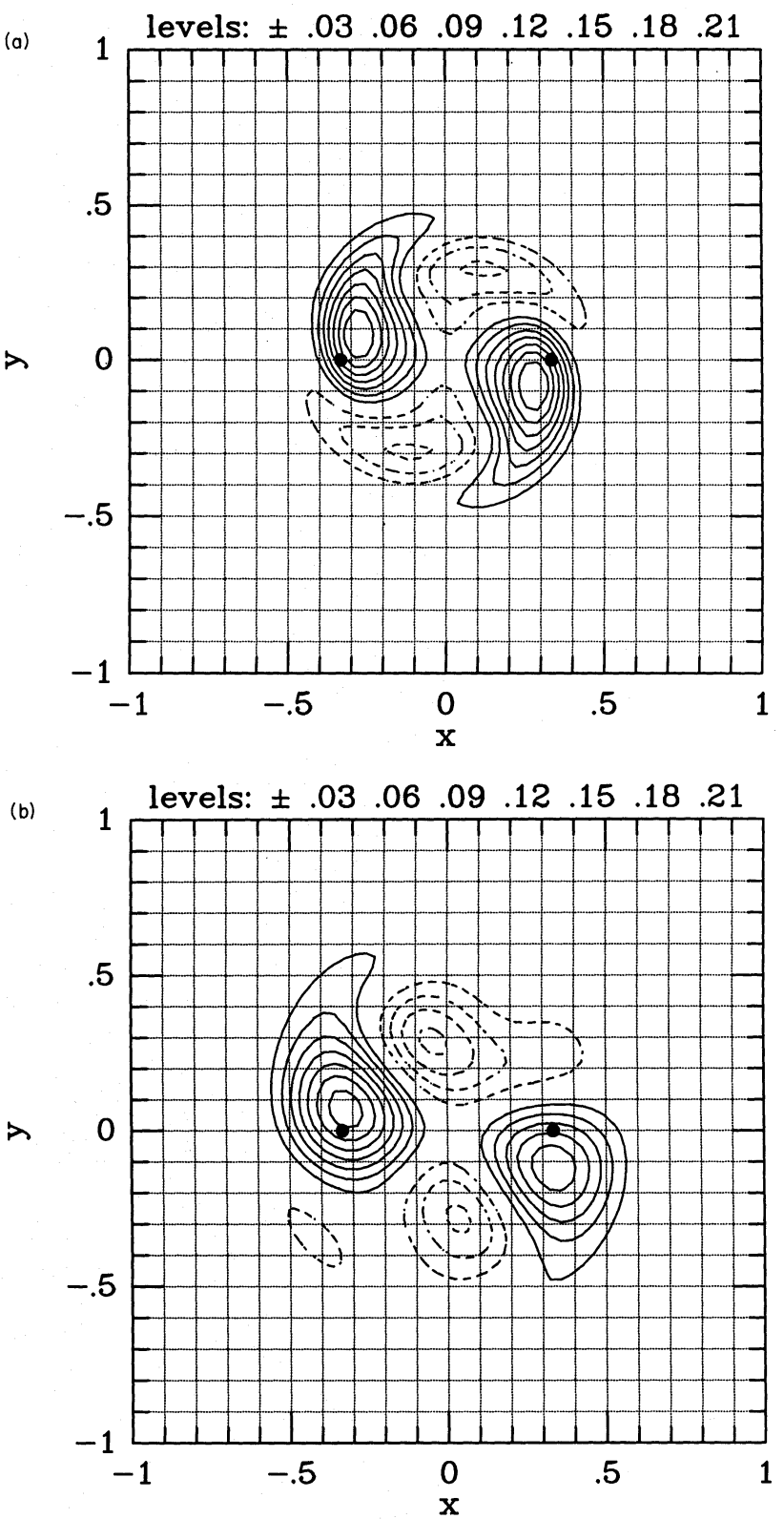

Figure 4. Wakes derived from (a) analytic calculation and (b) non-self-gravitating simulation involving two diametrically opposed satellites each of mass $m_s = 0.03$. Satellite positions are indicated by solid circles. The units and contour levels are as in Fig. 3.

collisionless systems, at least in some circumstances. (We defer a discussion of the efficiency of the hierarchical tree method relative to expansion techniques to Hernquist & Barnes 1989).

More importantly, both the anlaytic and numerical calculations give rather different sinking times, depending upon whether or not the response is treated self-consistently. According to Fig. 1, the self-gravity typically increases the decay time by a factor of ≈ 2–2.5. In the non-self-gravitating case, the effect of the self-consistent response on the evolution of the system is ignored, by definition. That is, suppose we expand the density and potential in perturbation series

$$\rho = \rho_0 + \rho_1 + \ldots \tag{7}$$

and

$$\phi = \phi_{\rm ext} + \phi_{\rm pri} = \phi_{\rm ext} + \phi_0 + \phi_1 + \ldots, \tag{8}$$

where $\phi_{\rm pri}$ is the potential of the primary, ρ_0 and ϕ_0 are the unperturbed terms, ρ_1 and ϕ_1 are the lowest-order corrections and $\phi_{\rm ext}$, which is of the same order as ϕ_1, is the potential of the satellite. Here ρ_i, which determines ϕ_i according to Poisson's equation, is the response to the potential perturbation ϕ_{i-1}. In the non-self-gravitating case, the contribution of ϕ_1 to the potential in the collisionless Boltzmann equation is to be ignored. The correct numerical procedure is to set the primary potential equal to the value that it would have *in the absence of the satellite.* That is, $\phi_{\rm pri} = \phi_0$ and the centre of the primary potential is to remain fixed in space, as if there were no perturbation present. Strictly speaking, then, the centre of mass shift is an aspect of the self-gravity of the response.

Modifications to the semi-restricted approach which include the motion of the centre of mass are, essentially, attempts to include the influence of higher-order terms in the potential expansion of the primary response, equation (8). It is not clear, *a priori*, that such procedures will yield meaningful results since the higher-order terms *distort* the potential as well as shift the centre of mass; this shift does *not* correspond to any single term in the perturbation series. Thus, the validity of these approximations must be justified on a case-by-case basis.

In summary, the analytic and numerical results presented here are in good agreement, when the effect of non-linear terms is taken into account. The orbital decay times of satellites around large galaxies is sensitive to the full self-gravitating response of the primary. The discrepancy between our conclusions and those of other recent numerical treatments apparently results from misuse of the term 'non-self-gravitating'.

Acknowledgments

We thank Simon White for stimulating discussion and Josh Barnes, Piet Hut, Scott Tremaine and an anonymous referee for useful comments on the manuscript. Supercomputer time was supplied through a grant provided by the Pittsburgh Supercomputing Center. MDW was supported in part by National Science Foundation grant AST-8802533 and LH was supported in part by New Jersey High Technology grant 88-240090-2.

References

Barnes, J., 1986. In: *The Use of Supercomputers in Stellar Dynamics,* p. 175, ed. Hut, P. & McMillan, S., Springer-Verlag, Berlin.

Barnes, J. & Hut, P., 1986. *Nature,* **324,** 446.

Bontekoe, Tj. R. & van Albada, T. S., 1987. *Mon. Not. R. astr. Soc.,* **224,** 349.

Chandrasekhar, S., 1943. *Astrophys. J.,* **97,** 255.

Hernquist, L., 1987. *Astrophys. J. Suppl.,* **64,** 715.

Hernquist, L., 1988. *Comp. Phys. Comm.*, **48,** 107.
Hernquist, L., 1989. *J. Comp. Phys.*, in press.
Hernquist, L. & Barnes, J., 1989. *Astrophys. J.*, submitted.
Lin, D. N. C. & Tremaine, S., 1983. *Astrophys. J.*, **264,** 364.
Tremaine, S., 1981. In: *The Structure and Evolution of Normal Galaxies,* p. 67, eds Fall, S. M. & Lynden-Bell, D., Cambridge University Press, Cambridge.
Weinberg, M. D., 1986. *Astrophys. J.*, **300,** 93.
Weinberg, M. D. 1989. *Mon. Not. R. astr. Soc.*, in press.
White, S. D. M., 1983. *Astrophys. J.*, **274,** 53.
Zaritsky, D. & White, S. D. M., 1988. *Mon. Not. R. astr. Soc.*, **235,** 289.